MULTI-BAND OPERATION OF A COMPACT H-SHAPED MICROSTRIP ANTENNA

Abdel Fattah Sheta,[1] Ashraf Mohra,[2] and Samir F. Mahmoud[3]
[1] Electrical Engineering Department
King Saud University
Riyadh 11421, Saudi Arabia
[2] Microstrip Department
Electronics Research Institute
Cairo, Egypt
[3] Electrical Engineering Department
Kuwait University
Safat 13060, Kuwait

Received 20 May 2002

ABSTRACT: *In this paper, a multi-band compact H-shaped microstrip antenna is studied. The resonant modes of the H-shaped structure are analyzed using the concept of electric and magnetic walls at the planes of symmetry. A flexible design approach that allows the pre-selection of the resonant frequencies of the antenna is described. Approximate design equations and curves are introduced and validated by simulated and experimental results. An H-shaped antenna is designed to support modes with resonance at 2.2, 2.8, 3, and 5 GHz. It is shown that dual-, triple-, or quad-band operation is possible by the proper location of a coaxial feed. Such antennas are implemented on duroid dielectric substrate with* $\varepsilon_r = 2.2$ *and* $h = 1.57$ *mm. The designed antennas are simulated by IE3D software and a good agreement with experimental results is demonstrated.* © 2002 Wiley Periodicals, Inc. Microwave Opt Technol Lett 35: 363–367, 2002; Published online in Wiley InterScience (www.interscience.wiley.com). DOI 10.1002/mop.10608

Key words: *microstrip antennas; miniature antennas; H-shaped; multi-band*

1. INTRODUCTION

Small-size multi-band microstrip antennas have attracted much attention due to the dramatic growth in wireless communications. Recently, several design approaches based on different structures have been proposed for single-feed dual-frequency operation. Capacitive loading of microstrip patch antennas has been proposed for dual-band operation [1], where the chip capacitor is used to reduce the antenna size [2]. Compact dual band planar inverted-F antennas (PIFA) have been reported in [3, 4], and are achieved with etched slots in the radiating element. The dual-band operation of small-size H-shaped patches with shorting pins has been proposed in [5]. Analysis has been performed using the finite difference time domain (FDTD) method. A triple-band antenna for GSM/DCS/GPS operation has been introduced in [6]. This antenna uses three resonant elements, with one for each band in special multi-layer arrangement. Several fractal antennas have been proposed to obtain multi-band operation [7, 8]. Although the proposed structure can be designed for three bands, the antenna has many resonances between the designed frequencies, which can increase the electromagnetic interference (EMI) in communication systems.

In an earlier investigation [9], a compact H-shaped antenna has been considered for a single-band operation. In this paper, we reconsider the H-antenna as a candidate for multi-band operation. To this end we first analyze the possible modes that can appear on the H-shaped structure on basis of electric and magnetic walls placed at the planes of symmetry. It is found that we can suppress some modes by proper feeding of the antenna. A feeding technique that permits the suppression of undesired modes is presented, followed by the introduction of an H-patch antenna designed to support four modes at 2.2, 2.8, 3, and 5 GHz. Experimental results of different types of antennas having the same geometry, but different feeder location, to operate on dual, triple, and quad bands are introduced and compared with theoretical predictions.

2. RESONANT FREQUENCIES AND RADIATION BEHAVIOR OF H-STRUCTURE

The resonant frequencies and radiation behavior of the H-structure as depicted in Figure 1(a) can be predicted from the possible current paths and distribution over the H-patch. Due to the symmetry of the structure on the X and Y axes, the concept of electric and/or magnetic walls placed at the two axes seems to be the most suitable approach to describe the nature of each mode and their radiation behavior. Placing electric and/or magnetic walls at the two axes results in the identification of four basic modes as shown in Figures 1 and 2. These modes can be divided into two families as described in the following subsections.

2.1 Modes With an Electric Wall Along the Y Axis

With an electric wall placed on the Y axis, we can identify two fundamental modes that will appear when an extra magnetic or electric wall lies along the X axis. The current distributions of these two modes are sketched in Figure 1(b) and (d), respectively. We shall denote the resonant frequencies of these two modes by f_{E0} and f_{E1}, respectively. The current flow in Figure 1(b), corresponding to a magnetic wall along the X axis, is maximum at the

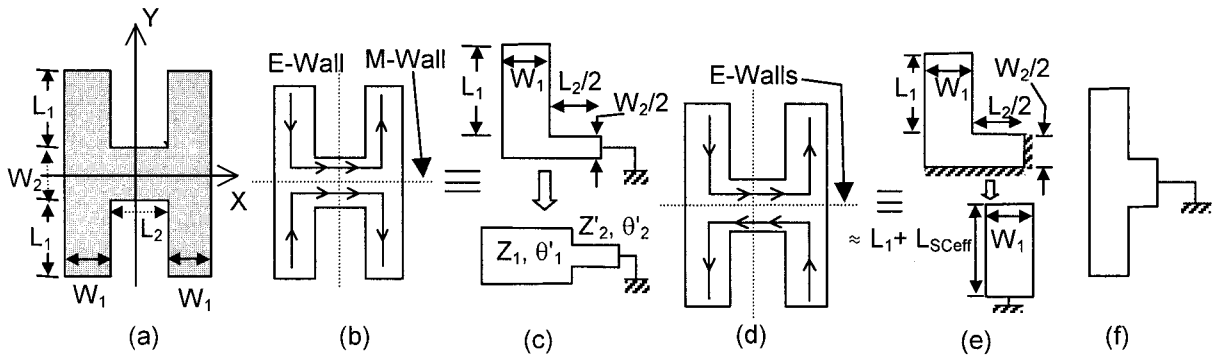

Figure 1 Current paths of possible modes with an electric wall along the Y axis (a) H-shape structure and its dimensions (b) Current path of the first mode with an electric wall along the Y axis and magnetic wall along the X axis (c) Equivalent circuit of Fig. 1(b). (d) Current path of the second mode with electric walls along the Y axis and along the X axis. (e) Equivalent circuit of Fig. 1(d) (f) Equivalent circuit based on TL theory that can be used to predict modes with an electric wall along the Y axis

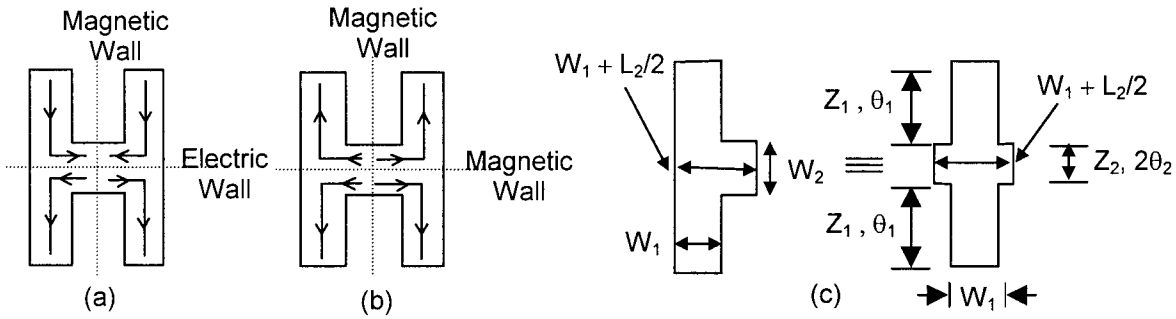

Figure 2 Current paths of possible modes with a magnetic wall along the *Y* axis (a) Current path of the first mode with a magnetic wall along the *Y* axis and electric wall along the *X* axis (b) Current path of the second mode with a magnetic wall along the *Y* axis and electric wall along the *X* axis (c) Equivalent circuit that can be used to predict the modes due to magnetic wall along the *Y* axis

center of the structure; thus its radiation characteristics can be approximated by a horizontal dipole. This mode, which is the lowest order mode, will appear when the mean path length of the current equals a half wavelength, given by

$$2L_1 + \frac{W_2}{2} + L_2 + W_1 = \frac{\lambda_{gE0}}{2} \tag{1}$$

Where λ_g can be considered as the guided wave wavelength of a microstrip line of width W_1. This approximation is valid as long as $W_2/2$ is close to W_1. More accurate calculation can be achieved if we consider the variation in the line width. In this case, the model parameters θ_1' and θ_2', shown in Figure 1(c), should be calculated in terms of the reference planes at the junction.

The resonant frequency of this mode (f_{E0}) can be calculated from the general relationship:

$$f = \frac{300}{\lambda_g \sqrt{\varepsilon_{eff}}} \text{ GHz}, \tag{2}$$

with λ_g in mm.

Next, consider the second mode corresponding to electric walls along the *X* and *Y* axes as shown in Figure 1(d). It is seen that the net current flow in the horizontal arm is almost zero due to the presence of the electric wall on the *X* axis. Therefore, this arm has little effect on the antenna properties. One can estimate the resonant frequency of this mode (f_{E1}) by assuming that the L_1 line is terminated by the parallel combination of two short-circuited lines, as suggested by Figure 1(e). The parallel combination of the two short-circuited lines has the effect of a short-circuited shorter line of width W_1 and effective length L_{SCeff}. In this case, resonance occurs when

$$4(L_1 + L_{SCeff}) = \lambda_{gE1}, \tag{3}$$

where L_{SCeff} is given by $L_{sceff} = (W_2/2)/[1 + Z_1W_2/Z_2'(W_1 + L_2)]$, where Z_1 and Z_2' are the characteristic impedances of microstrip lines of widths W_1 and $W_2/2$, respectively. This approximation is valid when $W_2/2$ and $L_2/2$ are small with respect to the wavelength ($W_2/2$ and $L_2/2 \leq \lambda/10$), which is satisfied in most practical cases. From Eqs. (1)–(3), f_{E0} and f_{E1} are related by

$$\frac{f_{E1}}{f_{E0}} = \frac{2L_1 + W_2/2 + W_1 + L_2}{2L_1 + W_2/(1 + Z_1W_2/Z_2'(W_1 + L_2)} \tag{4}$$

According to the current distribution shown in Figure 1(d), the radiation behavior of this mode can be assumed to resemble the radiation of two opposite vertical dipoles spaced horizontally by a distance $L_2 + W_1$. The equivalent circuit based on transmission line theory shown in Figure 1(f) can be used to predict the resonant frequencies f_{En} of higher order modes with $n > 1$.

2.2 Modes With a Magnetic Wall Along the Y Axis

In this section we study the modes that are identified by the presence of a magnetic wall on the *Y* axis. The resonant frequencies of these modes will be denoted by f_{Hn}, $n = 0, 1 \ldots$. The first mode is considered to have an electric wall along the *X* axis. The current flow in this case is mainly vertical, since the net current flow in the horizontal arm is zero. Thus, the antenna radiates as two vertical dipoles spaced horizontally by a distance $L_2 + W_1$. In this case the resonant frequency f_{H0} can be given by Eq. (3) with the proper value of L_{SCeff}. The equivalent circuit for this mode is a short-circuited line with length $W_2/2$ and width $W_1 + L_2/2$ connected at the end of the L_1 line. The short-circuited line here is effectively longer than the short-circuited line of Figure 1(e) and thus f_{E1} will be always greater than f_{H0}. However, the difference between f_{E1} and f_{H0} decreases as W_2 decreases. More accurate analysis of the modes of this family can be obtained by using the equivalent transmission line circuit in Figure 2(c).

The equivalent circuit in Figure 2(c) represents half of the H patch. It can be considered as three sections of cascaded transmission lines with different characteristic impedances and electrical lengths θ_1, $2\theta_2$, and θ_1 given by:

$$\theta_1 = \frac{\omega L_1}{c}\sqrt{\varepsilon_{eff1}}, \; 2\theta_2 = \frac{\omega W_2}{c}\sqrt{\varepsilon_{eff2}} \tag{5}$$

Z_1, θ_1, and ε_{eff1} are the characteristic impedance, electrical length, and effective relative dielectric constant, respectively, of a microstrip line of width W_1. Similarly, Z_2, $2\theta_2$, and ε_{eff2} are the characteristic impedance, electrical length, and effective relative dielectric constant of a microstrip line of width $W_1 + L_2/2$. The circuit behaves as a stepped impedance resonator (SIR) with $K = Z_1/Z_2$. In this case Z_1 is always greater than Z_2 and so K is greater than one. The admittance of the resonator from the open end is given by

$$Y_i = jY_2 \frac{2(K\tan\theta_2 + \tan\theta_1)(K - \tan\theta_1\tan\theta_2)}{K(1 - \tan^2\theta_1)(1 - \tan^2\theta_2) - 2(1 + K^2)\tan\theta_1\tan\theta_2} \tag{6}$$

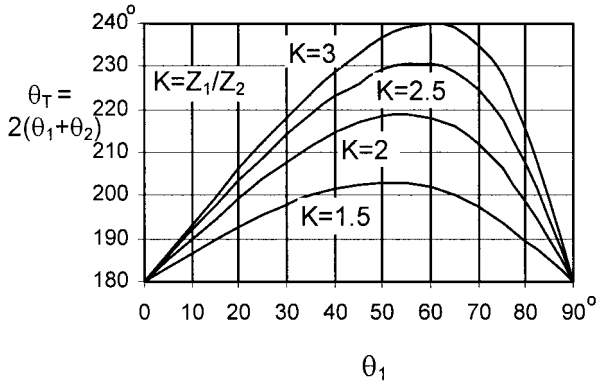

Figure 3 Resonance condition of SIR

The resonance condition can be obtained from $Y_i = 0$.

At the first resonance, f_{H0} (corresponding to a SC at the middle point), we get

$$K = \tan\theta_1 \tan\theta_2 \tag{7}$$

The resonator length, $\theta_T = 2(\theta_1 + \theta_2)$, can be plotted against θ_1 for different values of K as shown in Figure 3. This shows that resonance occurs when the total electrical length is greater than 180°. In this case the higher order responses appear at frequencies less than the harmonic frequencies and can be controlled using the appropriate choice of K.

At the first higher order mode with frequency f_{H1}, the following condition must be satisfied

$$K \tan\left[\theta_2\left(\frac{f_{H1}}{f_{H0}}\right)\right] = -\tan\left[\theta_1\left(\frac{f_{H1}}{f_{H0}}\right)\right] \tag{8}$$

where θ_1 and θ_2 are the electrical lengths at f_{H0}, and K is related to θ_1 and θ_2 by Eq. (7). f_{H1}/f_{H0} can be plotted against θ_1 for different values of K as shown in Figure 4. Note that singularities occur at some angles of Eq. (8). These should be avoided while selecting the values of K and θ_1.

The second higher order mode has f_{H2} given by

$$\frac{f_{H2}}{f_{H0}} = 1 + \frac{2\pi}{(\theta_1 + \theta_2)} \tag{9}$$

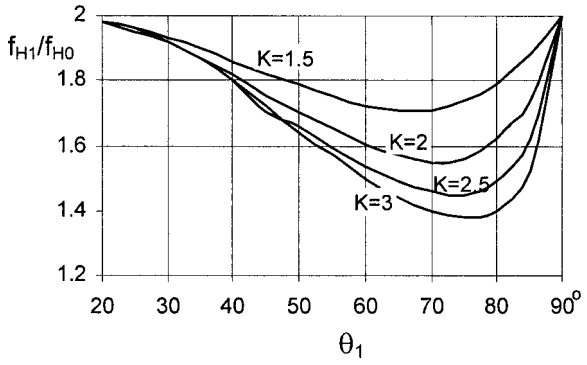

Figure 4 f_{H1}/f_{H0} against θ_1 for different values of K

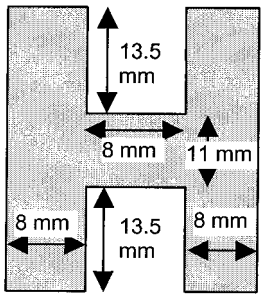

Figure 5 H-shaped antenna designed to support four modes. f_{E0}, f_{H0}, f_{E1}, and f_{H1} are 2.2, 2.8, 3, and 5 GHz, respectively. The substrate parameters are $\varepsilon_r = 2.2$ & $h = 1.57$ mm

The other higher order modes can be predicted using the equivalent circuit shown in Figure 2(c) as long as the quasi-TEM approximation is still valid.

3. MULTI-BAND OPERATION

We have seen that the geometry of the H-shaped antenna determines the resonant frequencies of the different modes. Thus, a choice of the dimensions L_1, L_2, W_1, and W_2 based on Eqs. (1), (3), (7), and (8) can be used to set the four resonant frequencies f_{E0}, f_{H0}, f_{E1}, and f_{H1} of the important modes. Alternatively, Eq. (4) and the curves shown in Figures (3) and (4) can also be used for the same purpose. This process can be easily used to set only two or three frequencies for dual- and triple-band operation.

Now, suppose we have an H-shaped antenna designed to support the first four frequencies. It has been observed that the location of the feed point has a strong influence on the impedance of the patch [10]. The FDTD method has been used to analyze the resonant modes of a conventional square patch for different feeding locations [11]. It is found that the symmetry of the feed determines the type of modes observed in the structures. In our case the modes are identified in terms of the electric and magnetic walls concept. From this definition, electric wall at a certain axis means zero impedance at any point along the axis; thus if we feed at any point where the impedance is zero for a given mode, this mode will not be excited. Therefore, the modes with an electric wall on the Y axis (with frequencies f_{E0} and f_{E1}), can be suppressed if we place the feeder at any point along this axis. Similarly, feeding at a point along the X axis will remove the modes with an electric wall along the X axis. These modes have resonance frequencies f_{H0}, f_{H2}, . . . or, generally f_{Hn} where n is an even number. Clearly, feeding right at the center of the H will suppress these two types of modes. For triple and quad bands, feeding close to any of the two axes should be avoided because low impedance is expected and at least two modes will be suppressed. The next example shows the proper locations for dual, triple, and quad bands.

4. DESIGN EXAMPLE

In order to demonstrate the multi-band operation of the H-shaped antenna described above, we introduce an H-shaped antenna designed to operate at 2.2, 2.8, 3, and 5 GHz. The above analysis shows that the lowest mode has resonant frequency f_{E0}, and that there are two modes with frequencies close to each other: f_{H0} and f_{E1}, where f_{E1} is always greater than f_{H0} and the difference between them decreases as W_2 decreases. The fourth mode resonates at f_{H1}. So the designed frequencies will be set as:

$$f_{E0} = 2.2 \text{ GHz}, f_{H0} = 2.8 \text{ GHz}, f_{E1} = 3 \text{ GHz and } f_{H1} = 5 \text{ GHz}.$$

TABLE 1 Comparison Between Theoretical, Simulated, and Measured Results

Resonant Mode Freq.	Theoretical Values		Simulation Using the IE3D Software				Measurements			
				Return Loss (dB)				Return Loss (dB)		
		Frq. GHz	Frq. GHz	Dual	Triple	Quad	Frq. GHz	Dual	Triple	Quad
f_{E0}	Eq. (1)	2.16	2.18			−7.5	2.19			−7
	Model (Fig. 1c)	2								
f_{H0}	Model (Fig. 2c)	2.9	2.75	−13	−12	−16.5	2.748	−13.5	−9.5	−10
f_{E1}	Eq. (3)	2.98	2.92		−8	−9.5	2.93		−9.8	−11
f_{H1}	Model (Fig. 2c)	5.13	5.02	−11	−15	−8.5	5.05	−10	−15.5	−8

Substituting f_{E0} and f_{E1} in Eqs. (1) and (3), we get

$$4L_1 + W_2 + 2L_2 + 2W_1 = \frac{136.4}{\sqrt{\varepsilon_{eff}}} \tag{9}$$

$$4L_1 + 4L_{SCeff} = \frac{100}{\sqrt{\varepsilon_{eff}}} \tag{10}$$

All lengths are in millimeters. Figures (3) and (4) are used to fix f_{H0} and f_{H1}. Since the frequency ratio $f_{H1}/f_{H0} = 1.78$, the horizontal straight line of a ratio 1.78 shown in Figure 4 can be used to find the possible values of θ_1, while in Figure 3, one finds the corresponding values of θ_2. This shows that there is no unique solution for f_{H0} and f_{H1}. However, this proves to be rather helpful and allows optimum dimensions that maintain the validity of Eqs. (9) and (10). Simultaneous solutions of Eqs. (7), (8), (9), and (10) can also be used in order to determine the patch dimensions. In this case, closed-form equations of the characteristic impedance as a function of line width, substrate thickness, and relative permittivity should be included. A tradeoff based on the first technique has been performed. Duroid dielectric substrate with $\varepsilon_r = 2.2$ and $h = 1.57$ mm is used. The H-dimensions are shown in Figure 5. Effects of open ends and discontinuities have been added. The H-patch is simulated by IE3D software for different feed locations. The simulated resonance frequencies are 2.18, 2.75, 2.92, and 5.02 GHz, which are very close to the theoretical values as shown in Table 1. The current distribution obtained from the simulation at the four resonance frequencies are shown in Figure 6. The current patterns are the same for all of the arbitrary locations of the feed point and in good accordance with the assumed currents for the different modes in Figures 1 and 2. This current distribution can be plotted for each mode by any appropriate feeding. Therefore, we use the current plots of all modes in order to find the appropriate feeding for dual, triple, and quad operations as described in the following subsections.

4.1 Dual Mode Operation

In this case two modes should be suppressed. As described above, feeding along the *Y* axis will suppress the two modes resonant at 2.18 and 2.92 GHz, i.e., f_{E0} and f_{E1}. Figure 7 shows the simulated and measured results of the H-shaped antenna with a coaxial feed on the *Y* axis and away from the lower edge by 0.5 mm. The frequency ratio is 1:81. Feeding at an appropriate point along the *X* axis, except at the center, is another solution. This suppresses modes having an electric wall at this axis (f_{H0} and f_{E1}). In this case, the highest frequency ratio, $f_{H1}/f_{E0} = 2.3$, is obtained. Simulation and measurements show that, feeding on the *X* axis and away from the center by 1.5 mm results on the observation of two resonant frequencies 2.18 and 5.05 GHz, which correspond to f_{E0} and f_{H1}, respectively. The measured return losses were 14 and 4 dB at 2.18 and 5.05 GHz, respectively. It is observed that simulation and measurements are quite close and agree well with theoretical results, as seen in Table 1.

4.2 Triple Mode Operation

As described previously, feeding near any of the two axes provides small impedance of two modes; thus this type of feeding should be avoided. Suppression of one mode can be achieved if we feed at a certain location where the current is almost zero for only one mode. In this case we can assume that this mode has very high impedance and will disappear, while the other modes will have a moderate matching. With the aid of the modal current distribution,

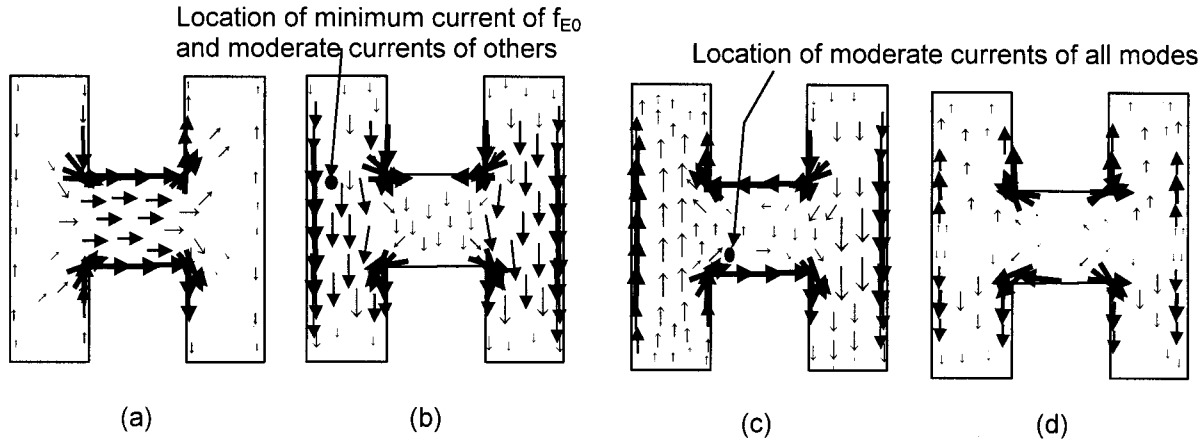

Figure 6 Current distribution, simulated by IE3D Zeland software, of the first four modes of the H-shaped antenna shown in Fig. 5. (a) Currents at $f_{E0} = 2.18$ GHz (b) Currents at $f_{H0} = 2.75$ GHz (c) Currents at $f_{E1} = 2.92$ GHz (d) Currents at $f_{H1} = 5.02$ GHz

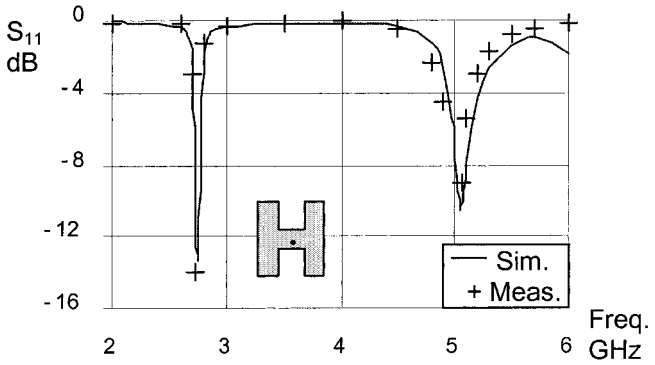

Figure 7 Simulated and measured results of H-shaped antenna fed to operate on dual-band f_{H0} and f_{H1}

a proper feed can be found where the current is minimum for f_{E0} and moderate for the others as shown in Figure 6(b). Feeding at this location leads to triple-band operation, as seen from the simulated and measured results in Figure 8.

4.3 Quad-Band Operation

Similar to the above case, the proper location for the quad-band operation should be away from the two axes and at a point where the currents of all modes are moderate. An appropriate location seems to be the one shown in Figure 6(c). The simulation and measurements given in Figure 9 show the excitation of the four modes. These measurements are in good accordance with the simulated results. Operation on dual- and triple-band can also be achieved by feeding at the quad-band location while designing for desired frequencies only. In this case, the appearance of undesired modes can increase the EMI between communication systems.

As we have described previously, feeding at the center point of the H suppresses the first three modes and keeps only the last one. This case has been verified by both simulation and measurements.

Agreement among theory, simulation, and measurements is observed from the comparisons in Table 1. The patch area is now about 40% of a conventional square patch designed at 2.2 GHz using the same substrate.

5. CONCLUSION

A new approach based on placing electric and/or magnetic walls at the planes of symmetry has been proposed to identify and analyze the normal modes of an H-shaped patch antenna. Design equations and curves have been provided. It has been found that the H-shaped structure can be designed to support up to four resonant

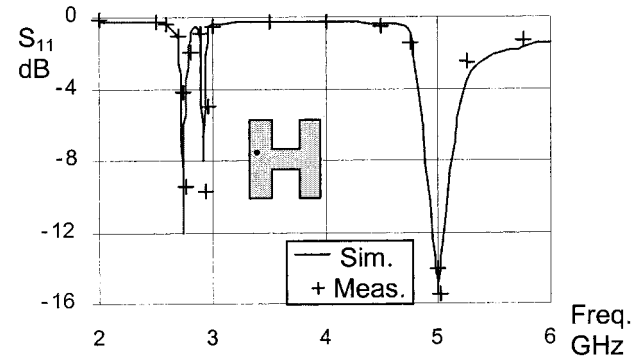

Figure 8 Simulated and measured results of H-shaped antenna fed to operate on triple-band f_{H0}, f_{E1}, and f_{H1}

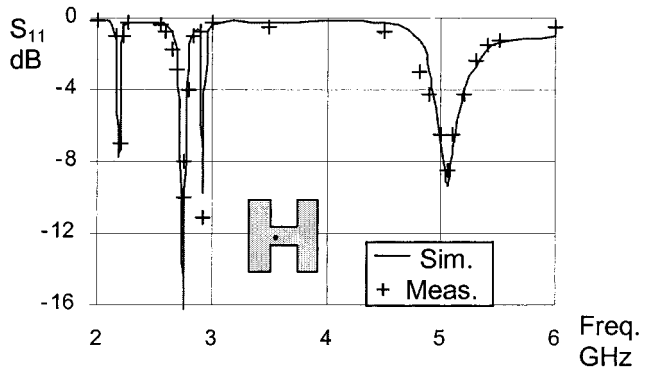

Figure 9 Simulated and measured results of H-shaped antenna fed to operate on four-band f_{E0}, f_{H0}, f_{E1}, and f_{H1}

modes and thus provide quad-band operation. However, the suppression of one, two, or three modes has been verified, which allows for the operation on dual and triple bands. Simulations have been performed using the IE3D software and the plots of the current distribution justify the proposed approach. Good agreement between theory and measurements has been achieved through the implementation of different antennas having the same dimensions and different feed locations to operate on dual, triple, or quad bands.

ACKNOWLEDGMENT

Dr. Samir F. Mahmoud thanks Kuwait University for providing him with a sabbatical leave during the academic year 2001–2002.

REFERENCES

1. G.S. Binoy, C.K. Aanandan, P. Mohanan, and K. Vadudevan, Square microstrip slot antenna with chip capacitor loading for dual frequency operation, IEEE AP-S Symp Dig 2001, vol. 4, pp. 90–93.
2. C.-S. Hong, Small annular slot antenna with capacitor loading, Electron Lett 36 (2000), 110–111.
3. C.R. Rowell and R.D. Murch, A compact PIFA suitable for dual frequency 900/1800-MHz operation, IEEE Trans Antennas Propagat 46 (1998), 596–598.
4. Z.D. Liu, P.S. Hall, and D. Wake, Dual-frequency planar inverted-F antenna, IEEE Trans Antennas Propagat 45 (1997), 1451–1458.
5. S.C. Gao, L.W. Li, T.S. Yeo, and M.S. Leong, A dual-frequency small microstrip antenna, IEEE AP-S Symp Dig 2001, pp. 86–89.
6. S.-T. Fang and J.-W. Sheen, A planar triple-band antenna for GSM/DCS/GPS operation, IEEE AP-S Symp Dig 2001, pp. 136–139.
7. R.V.H. Prasad, Y. Purushottam, V.C. Mistra, and N. Ashok, Microstrip fractal patch antenna for multi-band communication, Electron Lett 36 (2000), 1179–1180.
8. Z. Du, K. Gong, J.S. Fu, and B. Gao, Analysis of microstrip fractal patch antenna for multi-band communication, Electron Lett 37 (2001), 805–806.
9. A.F. Sheta, A novel H-shaped patch antenna, Microwave Opt Technol Lett 29 (2001), 62–65.
10. D.H. Schaubert and K.S. Yngvesson, Experimental study of a microstrip array on high permittivity substrate, IEEE Trans Antennas Propagat 1986, pp. 92–97.
11. E. Semouchkina, W. Cao, R. Mittra, and M. Langan, Effect of feeding symmetry on resonances in patch and capacitor structures, IEEE AP-S Symp Dig 2001, pp. 486–489.